Geotech Geol Eng (2021) 39:4963–4981
https://doi.org/10.1007/s10706-021-01806-y

ORIGINAL PAPER

Microstructural Analyses of Cement-Based Binders in Stabilizing Champlain Sea Clay

Moulay Youssef Monsif · Jinyuan Liu · Naresh Gurpersaud

Received: 17 July 2020 / Accepted: 5 April 2021 / Published online: 20 April 2021

Abstract This research investigated the strength development and the microstructural change in Champlain Sea clay when treated with five different cement-based binders. Champlain Sea clay, a marine clay, is commonly found in St. Lawrence Lowlands in eastern Canada. The unconfined compressive strength tests were conducted to measure the shear strength development of treated clay under different binder type, binder dosage, and curing time conditions. The scanning electronic microscopy (SEM) and X-ray diffraction (XRD) analyses were conducted to investigate the microstructural changes in the specimens. Based on the test results, it was found that cement is efficient to treat Champlain Sea clay with a significant strength improvement. For Champlain Sea clay used in this study, the optimum cement dosage was found to be around 100 kg/m^3 per mixed volume in terms of strength improvement and cost-effectiveness. The clay samples treated with a mix of cement and cement kiln dust and a mix of cement with slag showed a substantial strength increase over time. These results proved the feasibility of using cement kiln dust mix or slag to replace a portion of cement in treating Champlain Sea clay. Based on SEM observations, a substantial transformation was observed in the microstructure of the clay due to cement mixing. A large amount of clay-binder aggregates were formed and the hydration products filled the porous network of the clay samples, which results in a strength improvement in the treated clay. Based on the XRD analysis, hydration products, such as calcium silicate hydrate and calcium tecto-dialumodisilicate tetrahydrate, were formed in the cement-treated clay specimens, which explains the strength improvement of Champlain Sea clay due to cement mixing.

Keywords Champlain Sea clay · Marine clay · Deep soil mixing · Cement mixing · Ground improvement · Microstructural analysis · SEM · XRD

M. Y. Monsif
Ryerson University, Toronto, Canada
e-mail: mmonsif@ryerson.ca

J. Liu (✉)
Department of Civil Engineering, Ryerson University, 350 Victoria St., Toronto, ON M5B 2K3, Canada
e-mail: jinyuan.liu@ryerson.ca

N. Gurpersaud
Keller–North America, Acton, Canada
e-mail: NGurpersaud@keller-na.com

1 Introduction

Champlain Sea clay, also known as Leda clay, is commonly found along the St. Lawrence Lowlands regions in the provinces of Ontario and Quebec in eastern Canada (Penner and Burn 1978). It is one kind marine sediment formed about 8000–12,000 years ago

(Karrow 1961). The most well-known feature of Champlain Sea clay is its transformation from a relatively brittle material to liquid when it is disturbed (Crawford 1968). Destruction of the fabric of the clay may be due to induced stress or remolding. Weak particle bonds and high water contents are also the reasons behind its sudden change in state to fluid (Quigley 1983). Due to its peculiar properties, Champlain Sea clay is commonly subject to flow-type landslides (Gillot 1970), which resulted in property damages and loss of lives (Tavenas et al. 1971; Eden et al. 1971). Other engineering challenges include excess settlement over time and considerable shrinkage on dewatering (Penner and Burn 1978; Gillot 1970).

Ground improvement is normally required for construction in soft marine clays. Deep soil mixing (DSM), also known as cement mixing, shallow soil mixing, etc., is a popular ground improvement technique where the binder, normally cement or lime, is mixed in-situ with soil to improve its properties. The main objective of DSM is to improve the strength, stiffness, and permeability of the soil by creating bonding between soil particles. When soil is mixed with cementitious binders, the binder provides the necessary calcium ions to be exchanged with the monovalent cations such as Na^+ and K^+, which causes a significant reduction of the double layer thickness and hence a reduction in the plasticity along with an increase in shear strength. Cement hydration produces calcium silicate hydrate (CSH), calcium hydroxide, and also calcium aluminum hydrate (CAH) (Bergado et al. 1996). There are numerous research on the applications of DSM for treating difficult soils around the world (Okumura et al. 1972; Okumura and Terashi 1975; Terashi et al. 1980; Bergado et al. 1996; Miura et al. 2001; Åhnberget al. 2003; Lee et al. 2005; Shen et al. 2008; Horpibulsk et al. 2011; Liu et al. 2012; Kitazume et al. 2013; Sasanian and Newson 2013; Paniagua et al. 2019). Recently, there are some studies regarding the microstructural analysis of treated soils using advanced techniques, such as scanning electronic micrograph (SEM), X-ray diffractions (XRD), mercury intrusion porosimetry (MIP), and thermal gravity analysis (TGA). Al-Rawas et al. (2002) applied slag and cement/slag to treat an expansive Na-montmorillonite clay and found the formation of aggregations in the SEM analyses. Chew et al. (2004) and Kamruzzaman et al. (2009) investigated the development of microstructure in cement-treated Singapore marine clay by performing SEM and MIP analyses and concluded an increase in the degree of flocculation at higher cement dosages. Horpibulsuk et al. (2010) investigated the strength development in cement-stabilized silty clay from Thailand using SEM, MIP, and TGA and found an optimum water content at which cement is more effective in treating that clay. Du et al. (2014) investigated the changes in phases of major hydration products and microstructural characteristics of the zinc-contaminated kaolin clay treated with cement and found the major hydration reaction products formed at a low contamination. More recently, Liu et al. (2019) found a large number of ettringite and CSH crystals enwrapped in cement-treated Lianyungang marine clay and the changes in morphology and the amount of CSH with time by the SEM and XRD analyses. Cement is by far the most popular binder used in practice due to its readily availability. The cement dosages were reported to vary from about 100 kg/m^3 to 400 kg/m^3 for DSM projects around the world (Bruce et al. 2013). In addition to traditional cement or lime, other binders were also used in the studies, in particular the industry wastes. For example, Yoobanpot et al. (2017) compared the effect of cement, cement kiln dust (CKD), and CKD/fly ash on the strength and microstructures of the stabilized Bangkok clay. They found that cement led to a rapid increase in strength in the short-term curing period and tended to have a gradual increase in strength for the long-term curing period. However, the CKD-only mixture had the same trend as cement with a lower compressive strength.

There are only limited research available on the DSM technique in treating Champlain Sea clay. Locat et al. (1996) conducted a laboratory investigation on the quicklime stabilization of this clay. It was found that even at a higher water content above the liquid limit, a significant strength increase was obtained when enough time and lime were provided. More investigations have been recently conducted on the effectiveness of cement in treating this clay. Li et al. (2016) applied a cement dosage of 144 kg/m^3 and increased the unconfined compressive strength (UCS) of treated samples by 10 times that of the untreated ones. Afroz et al. (2018) investigated both strength and compressibility of general use Portland cement in treating Champlain Sea clay and found significant strength and compressibility improvement within a

short period of 7 days. However, there is no information regarding the optimum dosage of cement in treating Champlain Sea clay. The application of industry waste, like CKD, may also have significant economical and environmental benefits. In addition, it is also important to study the microstructural change due to the cement mixing and investigate the relationship between the microstructural change and strength improvement of the treated clay. This study was conducted to address these issues by investigating the efficiency of different cement-based binders and the associated microstructural changes using both SEM and XRD techniques. The binder used in this study include general use Portland cement and a mix of cement blended with either slag, CKD, or silica fume. The UCS test was used to investigate the strength development. The chemical reaction products were identified using the XRD technique. SEM was used to qualitatively evaluate the microstructural change in the treated clay specimens.

2 Design of Experimental Program

2.1 Champlain Sea Clay Samples Used in this Study

The Champlain Sea clay samples used in this study were obtained from a dam site approximately 60 km west from the city of Ottawa, Ontario, Canada. The soil samples were large size undisturbed Laval samples. Physical property tests were conducted on the clay sample, including the Atterberg limits, grain size, density tests (Liu et al. 2017). The detailed physical properties of Champlain Sea clay used in this study are shown in Table 1. According to the Unified Soil Classification System, the clay used in this study is classified as CH (Clay with high plasticity).

XRD was conducted on the same clay sample. The combined bulk and clay XRD results, consists mainly of illite clay with lesser amounts of quartz, chlorite, plagioclase feldspar, kaolinite, hornblende, potassium feldspar, and pyrite, as shown in Table 2.

2.2 Cement-Based Binders Applied in this Study

A total of five cement-based binders, obtained from a local cement manufacturing plant, were applied in this study: General use Portland cement (C), a mix of cement and CKD at a mass ratio of 1:1; a mix of cement and CKD (3:1); a mix of cement and slag (CS) (3:1); and a mix of cement and silica fume (HSF) (8% by weight).

CKD, a significant by-product of the cement manufacturing process, is a particulate mixture of partially calcinated and unreacted raw feed, clinker dust and ash, enriched with alkali sulfates, halides and other volatiles. Its size distribution, chemical, and physical properties depend on several production factors such as raw feed material, type of kiln operation, dust collection system, and fuel type. The use of CKD has been evaluated as an addition to Portland cement and found that CKD has a comparable effect on stabilizing expansive clay with similar results as Portland cement, fly ash, and lime (Zaman et al. 1992; Sayah 1993; Yala et al. 2012).

Blast furnace slag, a by-product during the conversion process of iron to steel, can be crushed or milled to very fine particles and make it a suitable partial replacement for or additive to Portland cement. The chemical composition of slag is quite uniform. It consists primarily of silicates, aluminosilicates, calcium-alumina-silicates, and some oxides such as iron oxide and manganese oxide (Yuksel 2018). Using slag in soil stabilisation is a cost-effective and environmentally friendly applications for this industrial by-product.

Silica fume, a by-product of the silicon smelting process, is known for its production of high-strength concrete. In the concrete industry, it is used for two different reasons: to replace a portion of the cement to reduce the cost; and as an additive to improve concrete properties under both fresh and hardened conditions. In this study, the use of silica fume is to investigate its effect on the strength development of soil–cement mixture.

The final strength of the treated soil is influenced by many factors, such as soil type, binder type, binder dosage, curing time, mixing method (Kitazume and Terashi 2013). According to a previous study on Champlain Sea clay by Li et al. (2016), a minimum dosage of 50 kg/m^3 per mixed volume was required to obtain a meaningful strength increase. Cement dosages ranging from 50 to 200 kg/m^3 were selected to see the impact of cement dosage in this study. The design of binder dosage was mainly based on the cement content, as shown in Table 3, where the type

Table 1 Physical properties of soil samples from a depth of 21.6 m

Sampling site	Arnprior, ontario
Depth below a 9-m weighting berm (m)	20–21
Unified soil classification system	CH
Grain size distribution (% finer): sand, silt, clay	2, 33, 65
Moisture content (%)	64–74
Liquid limit (%)	62–76
Plastic limit (%)	30–38
Specific gravity	2.65–2.70
Salinity (g/L)	15.53
Sensitivity	4–8
Activity, A	0.65–0.75
Undrained shear strength of undisturbed sample (kPa)	42
pH (-)	8.1

Table 2 Summary of XRD analysis on the clay sample used in this study (SNC-Lavalin 2017)

Type of Analysis	Weight (%)	Qtz (%)	Plag (%)	K-Feld (%)	Pyr (%)	Horn (%)	Clay (%)			Total clay (%)
							Kaol	Chl	Ill	
Bulk friction	50	20	13	5	4	7	3	10	38	51
Clay fraction	50	1	1	1	0	2	5	10	80	95
Bulk & clay	100	10	7	3	2	5	4	10	59	73

Abbreviations: *Qtz* quartz, *Plag* plagioclase feldspar, *K-Feld* potassic feldspar, *Pyr* pyrite, *Horn* hornblende, *Kaol* kaolinite, *Chl* chlorite, *Ill* Illite

Table 3 Summary table of binder types and dosages used in this study

Binder type	Mix ID	Cement dosage (kg/m^3)	Additive dosage (kg/m^3)	Test (number of samples)
C-General use Portland cement	C200	200	0	UCS(7) + SEM(3)
	C100	100	0	UCS(8) + SEM (3)
	C50	50	0	UCS(8) + SEM(3) + XRD (1)
HSF-cement-silica fume (12:1)	HSF50	46	4	UCS(6) + SEM(3)
CS-cement-slag (3:1)	CS67	50	17	UCS(7) + SEM(3)
CKD-cement-cement kiln dust (3:1)	CKD67	50	17	UCS(6) + SEM(3)
CKD-cement-cement kiln dust (1:1)	CKD100	50	50	UCS(7) + SEM(3)

UCS were conducted on samples cured at 7, 14, 28, 300 days, SEM on samples cured at 7, 14, 28 days, and XRD on 28-day cured samples only

and the number of samples for each test (bracketed) are also included in the table.

3 Soil Sample Preparation and Testing Procedures

3.1 Sample Preparation for UCS Samples

Both dry mixing and wet mixing methods are commonly used in practice, though dry mixing can be applied only to soils with natural water contents above 60% (Bruce et al. 2013). The wet mixing method following the procedures recommended by the US Federal Highway Administration Design Manual (Bruce et al. 2013) was used in this study. The detailed procedures can be found in Monsif et al. (2020).

The UCS test was conducted in accordance with ASTM D2166 standard. The load rate of 1.25 mm/min was applied to the sample and the test was terminated until a limit strain of 15% was reached.

3.2 Sample Preparation for SEM Specimens

The specimens for the SEM analyses were prepared from the same mix for the UCS samples. A 12-mm diameter by 10-mm high ring was used to host a SEM specimen. The soil-binder mix was pressed into the specimen ring and carefully trimmed to a flat surface. The specimen was then kept in a sealed plastic bag and cured under the same curing conditions as the UCS samples. After a desired curing time, the SEM specimen was oven-dried under a temperature of 105 °C for 24 h. Last, the specimen was polished with a sandpaper to a flat surface to be coated with a thin layer of gold. The coating is crucial for preventing charging of the specimen to obtain a high quality SEM image.

A JEOL-6380 LV SEM machine was used to obtain the SEMs of treated clay specimens under different binder and curing time conditions. The accelerating voltage ranged between 20 and 30 keV, with a working distance varying between 10 to 12 mm.

3.3 Sample Preparation for XRD Specimens

The XRD specimens were prepared the same way as the SEM specimens except a different specimen size of 35-mm in diameter and 7-mm in height and an air-dry procedure. The XRD analyses were performed using a PANalytical X'Pert Pro diffractometer equipped with a Cu-Kα X-ray tube. An input voltage of 45 kV and a current of 40 mA were used in this study. The specimens were scanned for 2 Theta values ranging from 5° to 90°, with a step length of 0.02°, a scanning rate of 2°/min, and a slit width of 0.3 mm. The XRD results were analyzed using X'Pert HighScore Plus software.

4 Test Results and Analysis

4.1 Change of Unconfined Compressive Strength Due to Cement-Mixing

The stress–strain curves of the UCS test of Champlain Sea clay before and after cement mixing are shown in Fig. 1. The average value of peak UCS, q_u, for three undisturbed clay samples was 84 kPa with a standard deviation of 6.0 kPa. The variation in the q_u was mainly caused by sample disturbance and test preparation. A significant strength improvement was observed after cement mixing. After mixing with a cement dosage of 50 kg/m^3, as shown in Fig. 1a, the average q_u of two tests for each condition increased substantially from 84 to 590 kPa in just 7 days. The q_u further increased with curing time to 842 kPa after 28 days of curing, approximately 12 times that of untreated soil. In addition to the strength increase, the failure strain, ε_f, reduced from around 3% to about 1%, which means that the failure mode of clay samples changed from a relatively ductile mode to a brittle one. The q_u of treated samples increased substantially with increasing cement dosage, as shown in Fig. 1b for 100 kg/m^3 cement dosage and Fig. 1c for 200 kg/m^3 dosage cases. For example, under the same curing period of 28 days, the q_u of treated samples increased from 842 kPa for 50 kg/m^3 samples in Fig. 1a, to 1948 kPa for 100 kg/m^3 samples in Fig. 1b, and further improved to 2472 kPa for 200 kg/m^3 samples in Fig. 1c. For cement-treated samples, the more prominent strength increase was observed when the cement dosage increased from 50 kg/m^3 in Fig. 1a to 100 kg/m^3 in Fig. 1b compared to the dosage increase from 100 to 200 kg/m^3 in Fig. 1c. This may imply the optimum cement dosage would be around 100 kg/m^3 in terms of strength increase and cost effectiveness. The q_u also increased with increasing curing time. For the 100 kg/m^3 samples in Fig. 1b, the q_u increased

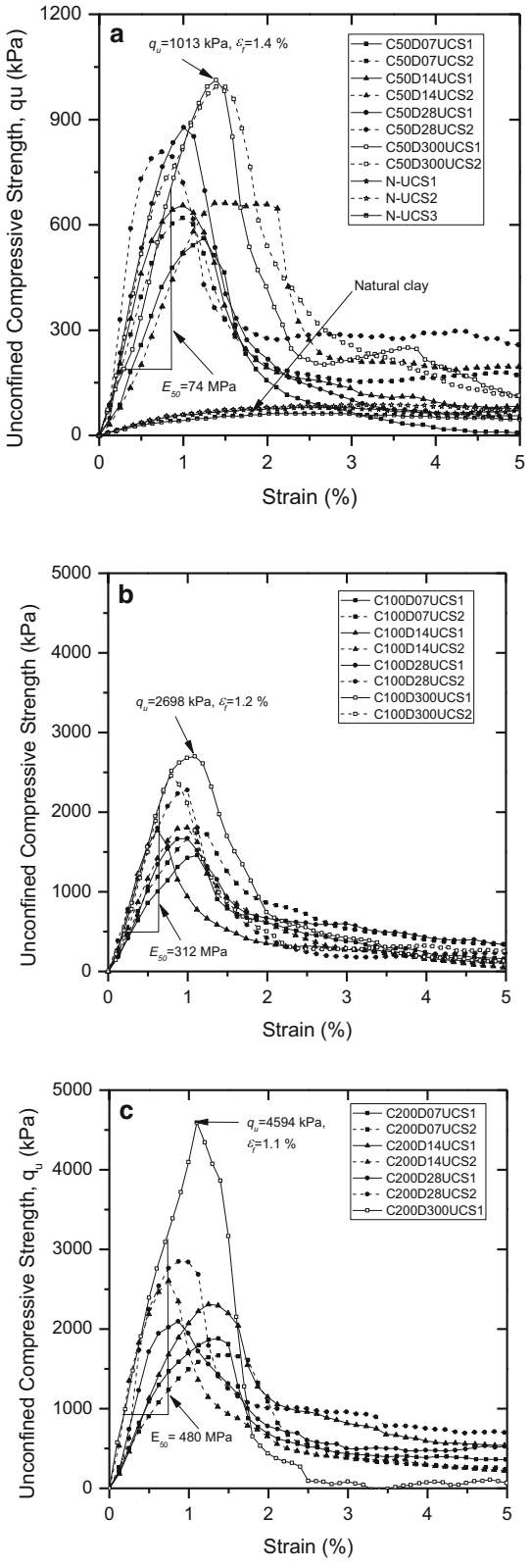

◀**Fig. 1** The stress–strain curves of unconfined compressive strength tests on Champlain Sea clay without and with cement treatment **a** 50 kg/m^3; **b** 100 kg/m^3; **c** 200 kg/m^3

substantially from 1948 kPa at 28 days of curing to 2578 kPa at 300 days. The strength increase of Champlain Sea clay due to mixing is similar to findings in other soils (Kawasaki 1981; Lorenzo and Bergado 2006).

The stress–strain curves of clay samples treated with other cement-based binders are similar to those of cement-treated samples, but with different magnitudes of q_u, as shown in Fig. 2a for CKD 67 kg/m^3 dosage cases, Fig. 2b for CKD 100 kg/m^3 dosage cases, Fig. 2c for HSF 50 kg/m^3 dosage cases, and Fig. 2d for CS 67 kg/m^3 dosage cases. The samples treated with other cement-based binders became more rigid as curing time increased. For example, the ε_f reduced from 1 to 2% for curing times up to 28 days to around 0.5% at the curing time of 300 days. The effect of the curing time on the q_u values is shown in Fig. 3 for different binder types, where q_u is the average value of two samples tested for each curing and binder condition. Generally, the q_u value increased with increasing curing time. The q_u value is mainly controlled by the cement dosage at the short curing time. For example, a very similar q_u was found among different binder samples at the short curing time up to 28 days under the same cement dosage (50 kg/m^3 except 46 kg/m^3 for HSF samples in Fig. 2c) even with different additive conditions. With the increasing curing time, the increase of strength over time became more prominent in samples treated with the cement/slag mix (Fig. 2d) or the cement/CKD mix (CKD100 in Fig. 2b). The q_u values from these two binder types were much higher than the C50 samples, which means CKD and slag can help pozzolanic reactions. These results show the feasibility and efficiency of using CKD or slag to replace a portion of cement in treating Champlain Sea clay. More details about the UCS test results can be found in Table 4.

The plot of q_u against the ratio of total water content to binder content, *w/c*, is shown in Fig. 4, where q_u reasonably follows a function of w/c at a certain curing time. The *w/c* parameter was first proposed by Miura et al. (2001) to represent the strength behavior of cement-stabilized clay. This q_u change with *w/c* for treated Champlain Sea clay is similar to the trends

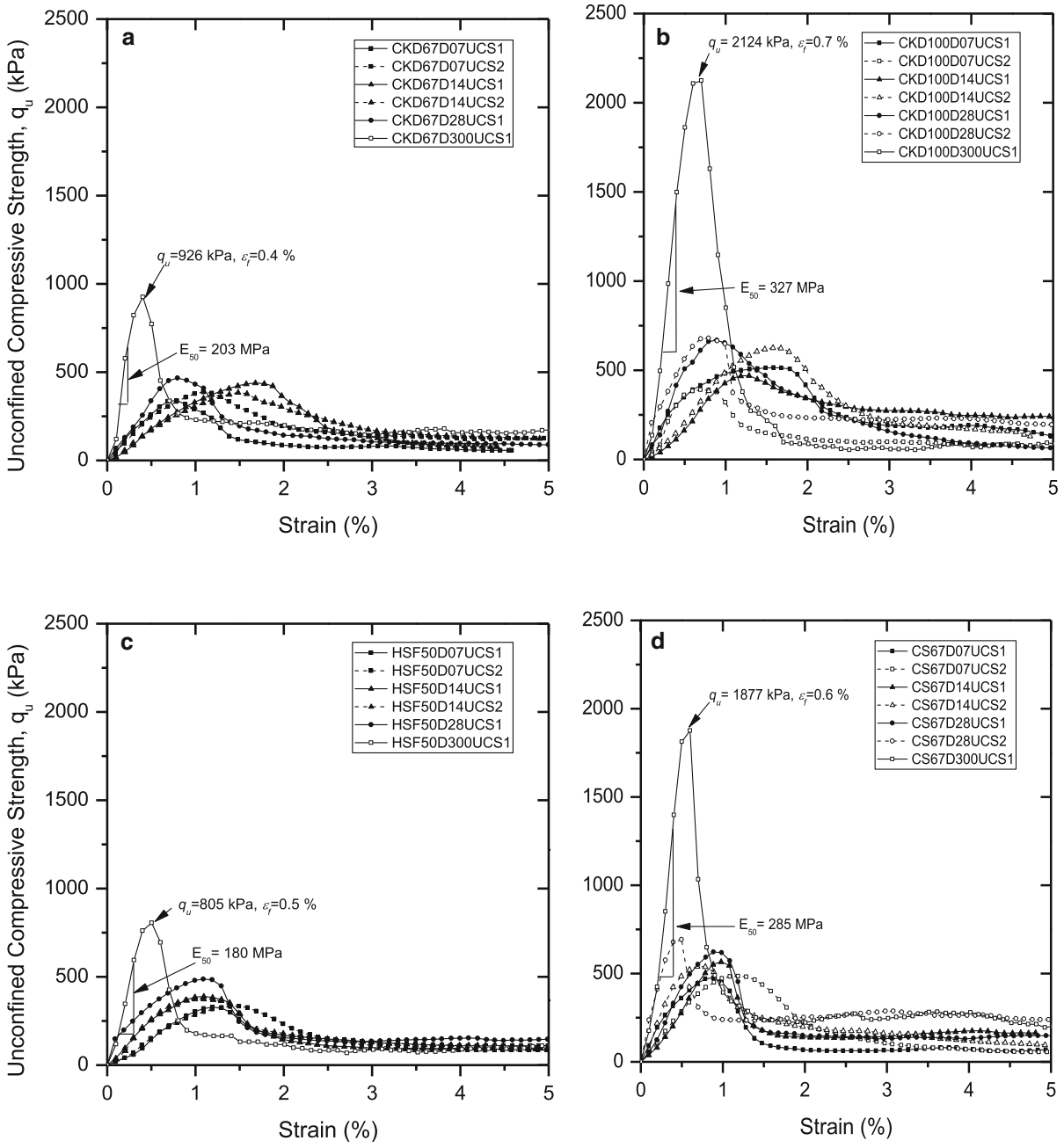

Fig. 2 Stress–strain curves of unconfined compressive strength tests on Champlain Sea clay treated with other cement-based binders

found in other soils (Terashi 1977; Lorenzo and Bergado 2004).

The secant moduli, E_{50}, was determined at a stress level at the half of the q_u, as illustrated in Figs. 1 and 2. The relationship between E_{50} and q_u of each sample is shown in Fig. 5. The figure demonstrated that the E_{50} of treated Champlain Sea clay almost linearly increased with the q_u regardless of different binder types and curing period. The E_{50} can be taken as 70 q_u–180 q_u, with an average ratio of 123 for cement-treated Champlain Sea clay. This ratio of E_{50}/q_u for treated Champlain Sea clay is within the lower range reported on mixing treated soils, as shown in Table 5.

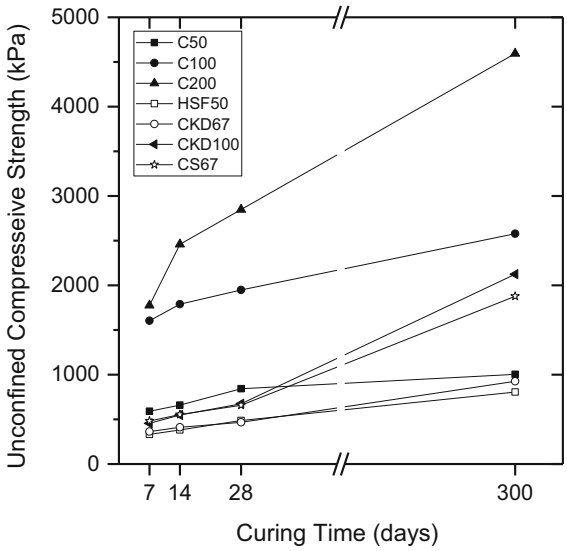

Fig. 3 Effect of curing time on the q_u of treated Champlain Sea clay

A non-destructive test was performed using a Pundit Lab ultrasonic NDT device on the cement-treated samples. Frequency of transmission pulses was kept at 50 kHz and travel time at the microsecond level was read directly on the screen of the device. The ultrasonic pulse velocity was calculated by dividing the sample length by the travel time for the ultrasonic pulses. Previous studies showed that the relationship between the ultrasonic velocity and q_u can be estimated by an exponential relationship proposed by Ravindrarajah (1997). The correlation between the ultrasonic pulse velocity, v, and q_u is shown in Fig. 6. The close relationship is similar to the finding for cement-treated sand by Choobbasti and Kutanaei (2017). This verifies the possibility of applying ultrasonic NDT to assess the strength of cement-treated Champlain Sea clay. More research is required in the future to confirm this finding.

4.2 Microstructural Change of Champlain Sea Clay Due to Cement Mixing

The elemental composition analysis of the natural clay was conducted using energy dispersive spectroscopy (EDS) technique. The average composition of a specific area (Spectrum 6 in Fig. 7a) is shown in Fig. 7b. This area is composed mainly of sodium (Na) and chlorine (Cl) with about 37.6% by weight. The high amount of sodium and chloride can be attributed to the marine sedimentation environment of Champlain Sea clay.

The microstructure of a natural clay specimen was observed on a view parallel to its bedding plane using the SEMs under two magnifications of 5000 (Fig. 8a) and 10,000 (Fig. 8b, c). The observed structure is an aggregated structure with the aggregate diameter of approximately 1–2 μm. The aggregates are composed of small platelets separated by a porous network. Some silt particles are scattered among the aggregates. Figure 8b highlights a silt particle with a diameter of around 6 μm, to which some platelets are stuck by the side and the edge. The texture of the natural clay consisted of many sheet-like particles (Fig. 8c). The flaky and plate-like particles could be identified as illite with some scattered kaolinite minerals. The sample exhibits a matrix of overlap between particles where slightly curled flakes arises (Fig. 8c).

The impact of cement mixing on the microstructure of the clay is shown in Fig. 8d and f. Microstructure of the 7-day cured specimen (Fig. 8d) did not show a significant difference from the natural one mainly due to short curing time. However, with increasing curing time, the hydration products clearly change the microstructure of the cemented specimens. The soil clusters and the pores were covered and filled by the hydration products at 14 day curing (Fig. 8e). Over time, the hydration products in the pores became more prominent and the soil–cement clusters became larger because of the growth of cementitious products over time (Fig. 8f). No significant change can be easily observed between the 14-day and the 28-day cured specimens, which is in agreement with the similar q_u values, as shown in Table 4. This could be due to the insufficiency of cement for further hydration after 14 days of curing.

The effects of cement dosage on the pore size distribution of the cemented specimens are shown in Figs. 8 and 9. An early formation of hydration products was observed in the 7-day cured specimens under higher cement dosages (Fig. 9a and d). Substantial growths of reaction products can be observed as the curing time increased to 14 days (Fig. 9b and e), where cementitious bridges in the form of needle-like crystals, also called ettringite (marked by rectangles) are formed between clay aggregates and clay particles. In the 28-day cured specimens (Fig. 9c and f), substantial pores were closed and more hydration products were hardened on the surface of the clay

Table 4 Summary of unconfined compressive strength tests conducted on natural and treated Champlain Sea clay samples

Sample ID	q_u (kPa)	ε_f (%)	γ_d (kg/m^3)	w_c (%)	$E_{50\ (MPa)}$	Sample ID	q_u (kPa)	ε_f (%)	γ_d (kg/m^3)	w_c (%)	E_{50} (MPa)
N-UCS1	87	2.88	865	77.93	7.44	HSF50D07UCS1	329	1.19	852	72.07	28.86
N-UCS2	79	2.32	865	77.93	7.28	HSF50D07UCS2	334	1.49	846	73.50	31.01
N-UCS3	62	2.02	865	77.93	5.63	HSF50D14UCS1	389	1.09	851	73.93	52.36
C50D07UCS1	561	1.24	873	71.84	59.57	HSF50D14UCS2	374	0.99	852	73.32	51.01
C50D07UCS2	620	0.99	865	72.80	76.63	HSF50D28UCS1	487	1.09	858	73.72	104.53
C50D14UCS1	656	0.99	871	71.93	82.11	HSF50D300UCS1	805	0.50	NA	NA	170.99
C50D14UCS2	663	1.37	874	71.57	45.33	CS67D07UCS1	476	0.88	880	71.01	98.35
C50D28UCS1	877	1.00	860	73.83	105.25	CS67D07UCS2	486	1.18	877	70.22	58.53
C50D28UCS2	808	0.74	869	73.09	133.09	CS67D14UCS1	567	0.98	893	70.50	56.33
C50D300UCS1	1013	1.39	875	74.28	73.93	CS67D14UCS2	540	0.69	891	69.98	110.78
C50D300UCS2	994	1.39	871	75.98	100.27	CS67D28UCS1	622	0.89	886	72.15	74.93
C100D07UCS1	1460	1.12	871	70.61	171.94	CS67D28UCS2	693	0.50	896	72.17	16.87
C100D07UCS2	1748	1.11	877	67.73	203.25	CS67D300UCS1	1877	0.55	NA	NA	285.33
C100D14UCS1	1772	0.61	870	70.90	303.94	CKD67D07UCS1	338	0.79	851	73.77	61.19
C100D14UCS2	1806	0.99	869	71.02	234.87	CKD67D07UCS2	387	1.09	856	72.88	51.28
C100D28UCS1	1670	0.99	868	71.77	188.15	CKD67D14UCS1	438	1.68	857	68.64	35.87
C1000D28UCS2	2227	0.99	872	71.39	314.39	CKD67D14UCS2	385	1.48	865	69.48	34.63
C100D300UCS1	2698	1.09	869	73.85	311.45	CKD67D28UCS1	466	0.80	876	74.05	63.33
C100D300UCS2	2457	0.79	884	72.99	294.01	CKD67D300UCS1	926	0.40	NA	NA	202.75
C200D07UCS1	1881	1.37	862	72.06	219.49	CKD100D07UCS1	514	1.58	829	77.43	84.15
C200D07UCS2	1670	1.49	881	70.77	191.49	CKD100D07UCS2	398	0.69	822	75.55	41.29
C200D14UCS1	2312	1.24	876	72.70	227.20	CKD100D14UCS1	470	1.28	838	74.83	36.44
C200D14UCS2	2606	0.74	877	72.71	439.15	CKD100D14UCS2	626	1.57	848	74.70	44.23
C200D28UCS1	2096	0.86	863	72.70	299.22	CKD100D28UCS1	669	0.89	845	75.03	90.88
C200D28UCS2	2848	0.87	881	72.06	251.61	CKD100D28UCS2	680	0.79	843	76.40	146.93
C200D300UCS1	4594	1.09	871	74.94	480.95	CKD100D300UCS1	2124	0.65	NA	NA	327.07

q_u, peak unconfined compressive strength; ε_f, failure shear strain corresponding to q_u; γ_d, dry unit weight of sample before the UCS test; w_c, water content of the sample measured after UCS test; E_{50}, secant shear modulus at the stress level at the half of q_u

particles. These hydration products bind together the clay particles or clusters of clay particles and created a stronger soil–cement matrix of soil. With increasing cement dosage, the cementitious products fill small pores and formed large soil–cement clusters at 7-day curing. With increasing curing time, the volume of small pores decreased and more cementitious products formed larger aggregates and interconnected the particles together.

It is worthy noting that the poor quality of SEM micrographs were observed for treated clay specimens compared to natural clay specimens. The 24-h oven-drying method might leave a high amount of water inside the treated clay specimens, which could cause this image quality issue. This issue became less prominent in the specimens by increasing curing time and cement dosage, which allows more consumption of water for hydration reactions and reduces the charging effect for a better image quality. In addition, the liquid nitrogen freezing method used by other researchers shall be investigated to improve the quality of SEMs in the future studies.

The SEM micrographs of specimens treated with two CKD dosages are shown in Fig. 10. For CKD67 specimens, Fig. 10a–c show quite similar surface morphology without many soil-binder aggregations

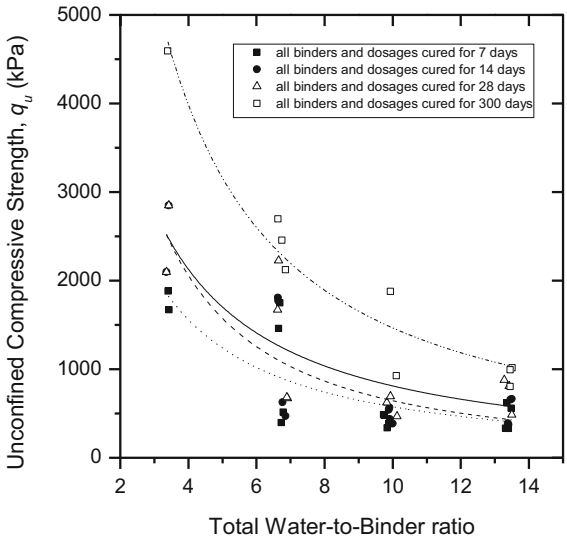

Fig. 4 Unconfined compressive strength q_u versus the total water to binder ratio

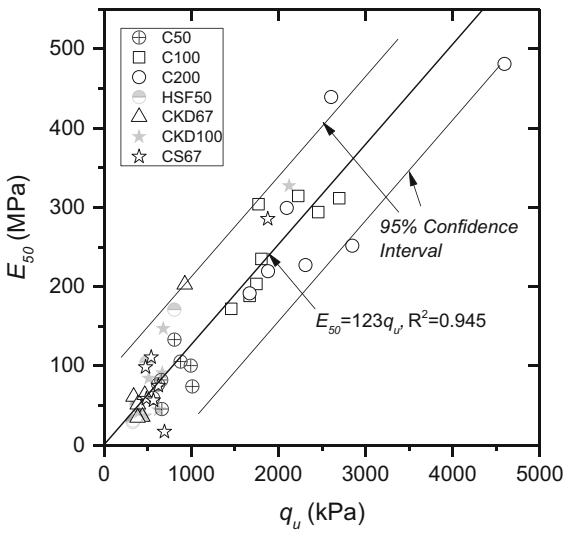

Fig. 5 Modulus of elasticity versus unconfined compressive strength of different cement-based binder treated Champlain Sea clay

formed under different curing times. The main reason can be contributed to insufficient cement to generate enough cementitious reactions. This was also associated with similar q_u values obtained in the UCS tests. With the CKD dosage being increased, a significant amount of large soil-binder aggregates was observed in the SEMs of CKD100 specimens. At the curing time of 7 days, the clay particles started to get coated with the hydration products. As the curing time increased, a large amount of aggregate clumps in the size of approximately 5 μm started to get formed (indicated by the yellow ellipse in Fig. 10e), in particular, in the 28 day-cured specimen (Fig. 10f).

The SEM micrographs of CS67 and HSF50 specimens are shown in Fig. 11. Significant changes could be observed with increasing curing time in the microstructures of CS67 specimens (Fig. 11a–c). At the 7-day curing, the clay particles were coated by the early stage formation of the hydration products and resulted in a reduction in voids in the CS67 specimen (Fig. 11a), while not much found in the HSF50 specimen (Fig. 11d). As the curing time increased to 14 days, the clay-binder aggregates were observed in the SEMs of both the CS67 and HSF50 specimens (Fig. 11b and e). At the curing time of 28 days, these aggregates grew further to about 7 μm in length in the CS67 specimen (Fig. 11c) and about 6 μm in length in the HSF50 specimen (Fig. 11f), which are about three times that of natural clay. Besides the aggregations, the aggregate interlock was observed in the SEMs, which could be another mechanism for the shear strength improvement. These microstructure changes also explain the mechanism behind the q_u increase obtained in the UCS tests.

In summary, the SEM micrographs of the treated specimens show both hydration products and cementitious products significantly increased over time, though the intensities of the changes varied depending on the types of binder and dosage. The hydration products and cementitious products not only fill the pore space but also enhance the inter-aggregate bonding strength, which result in an increase in the shear strength. Based on the microstructural analysis, a cement dosage of 50 kg/m^3 is required to show the microstructural change and cementitious product growth over time. With additives, more hydration products and cementitious products were observed in the treated clay specimens. The significant microstructure changes observed in the CKD100 (Fig. 10d–f) and CS67 (Fig. 11a–c) specimens also correlated well with the substantial strength increase over time in these samples observed in the UCS tests. The microstructure analysis confirmed the feasibility and efficiency of using CKD or slag to replace a portion of cement in treating Champlain Sea clay.

Table 5 The value of E_{50}/q_u for various soil-binder samples

E_{50}/q_u	Soil type and mixing details	References
70–180	Champlain Sea clay, cement-based binders, wet mixing	This study
115–150	Bangkok clay, cement, wet mixing	Lorenzo and Bergado (2006)
350–1000	Tokyo, Chiba, Kanagawa, Aichi, Osaka, Mie and Fukuoka clays, cement, wet mixing	Kawasaki (1981)
50–180	Gyttia clay (Sweden), Lime and cement, dry mixing	Baker (2000)
30–300	Silty clay and silty sand (Taiwan), Cement, wet mixing	Fang (2001)

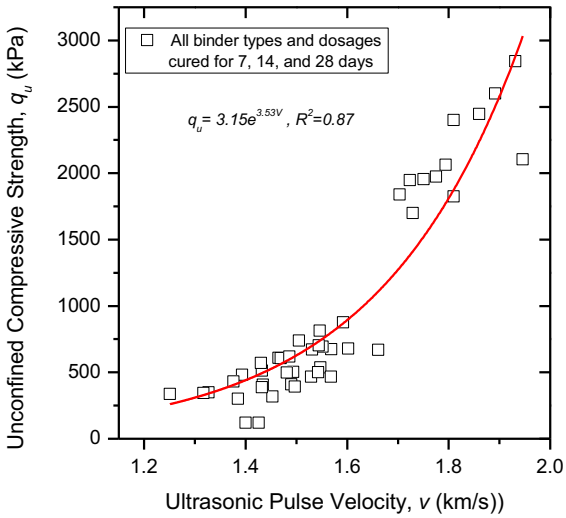

Fig. 6 The ultrasonic pulse velocity and q_u of cement-treated Champlain Sea clay

4.3 XRD Analysis of Phase Composition Change Due to Cement Mixing

The XRD patterns indicated that the dominant minerals for natural clay are illite ($2K_2O.\ 3MgO.\ Al_2O_3.\ 24\ SiO_2.\ 12H_2O$), kaolinite ($Al_2O_3.\ 2SiO_2.\ 2H_2O$), and quartz ($SiO_2$), as shown in Fig. 12a. After cement mixing, more phases were observed in the cement-treated specimen, as shown in Fig. 12b, where the specimen was mixed with 50 kg/m^3 cement and cured for 28 days. The major reaction products were identified as calcium silicate hydrate (CSH, $Ca_{1.5}SiO_{3.5}.H_2O$) and tecto-dialumodisilicate tetrahydrate (CASH, $CaAl_2\ Si_2O_8\ (H_2O)_4$). Calcium hydroxide ($Ca(OH)_2$), a major product of cement hydration, could not be detected in the treated-clay specimen cured at 28 days because of its rapid dissolution as Ca^{2+} and $(OH)^-$ into pore solutions after cement hydration, which leads

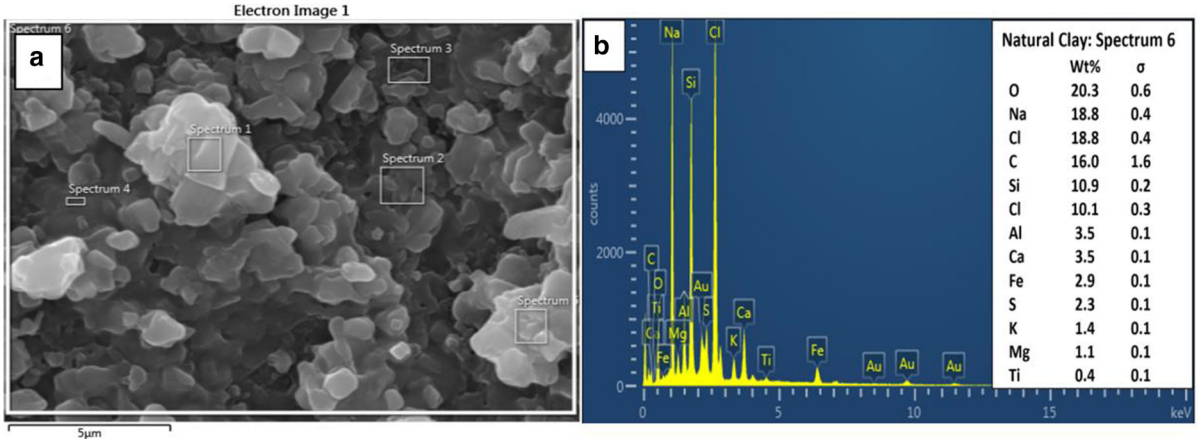

Fig. 7 Spectra of EDS analysis (**a**) and average elemental composition of natural clay (**b**)

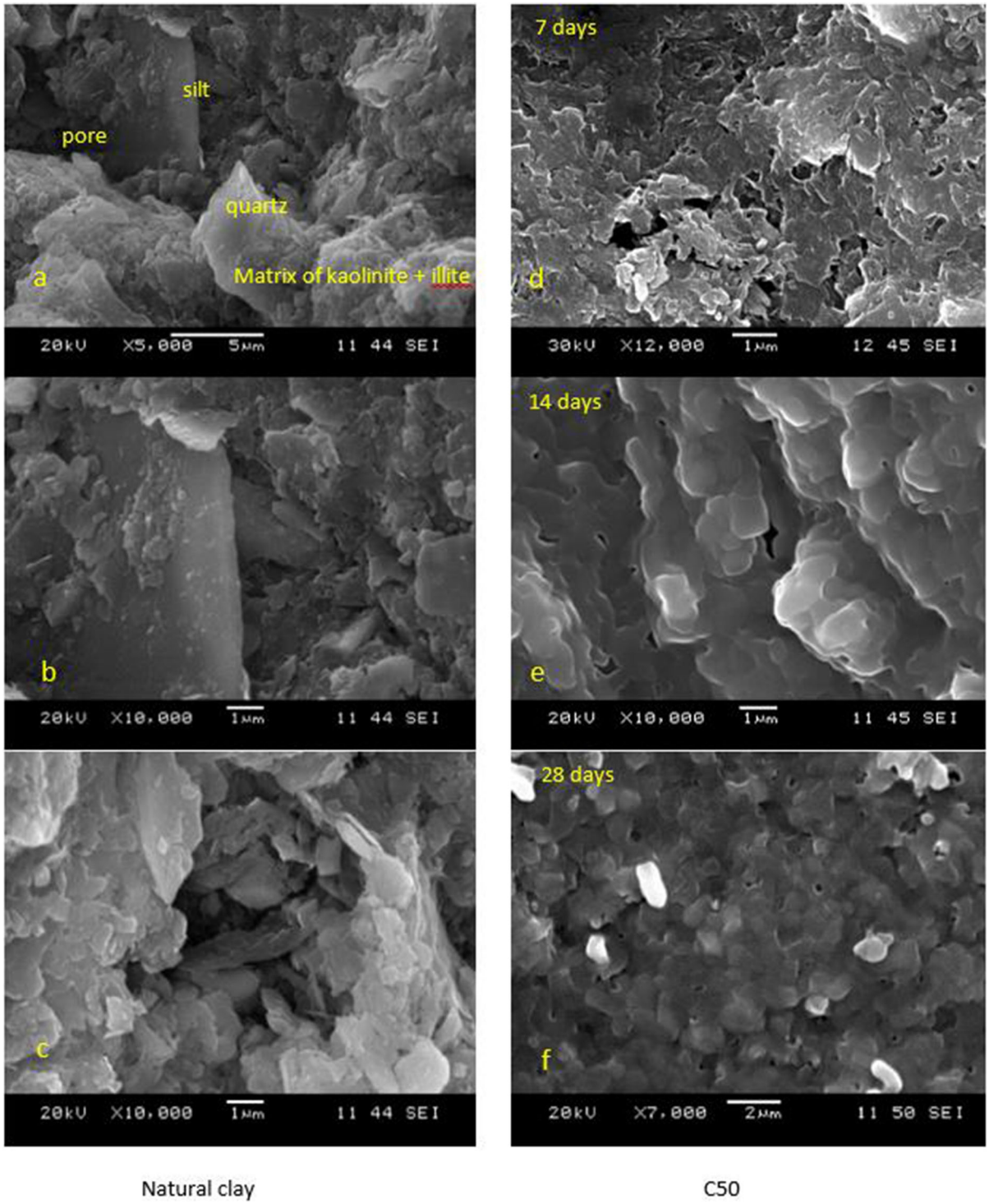

Fig. 8 SEM micrographs of natural clay and clay treated with 50 kg/m^3 cement

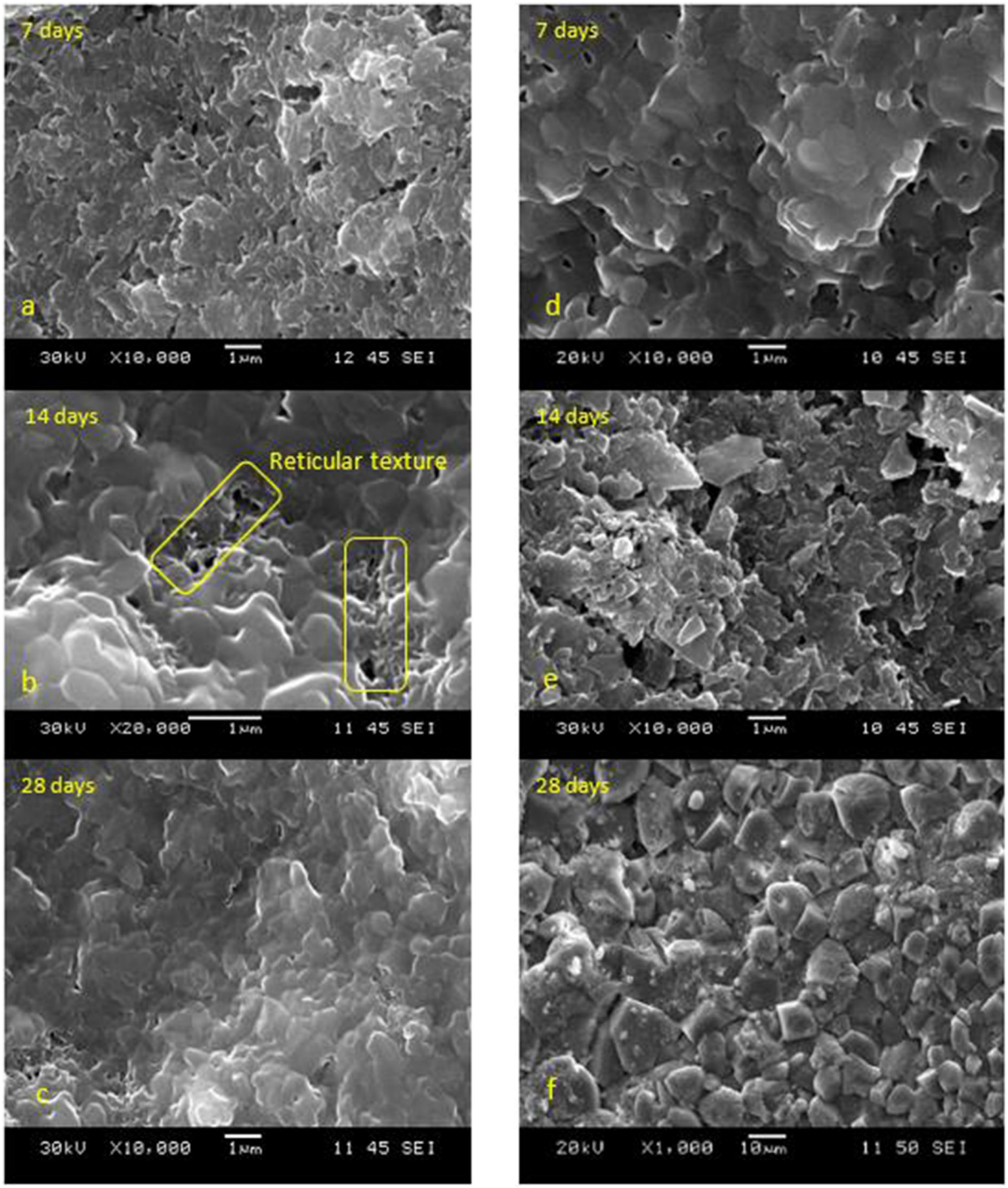

Fig. 9 SEM micrographs of clay specimens treated with cement dosages of 100 and 200 kg/m^3

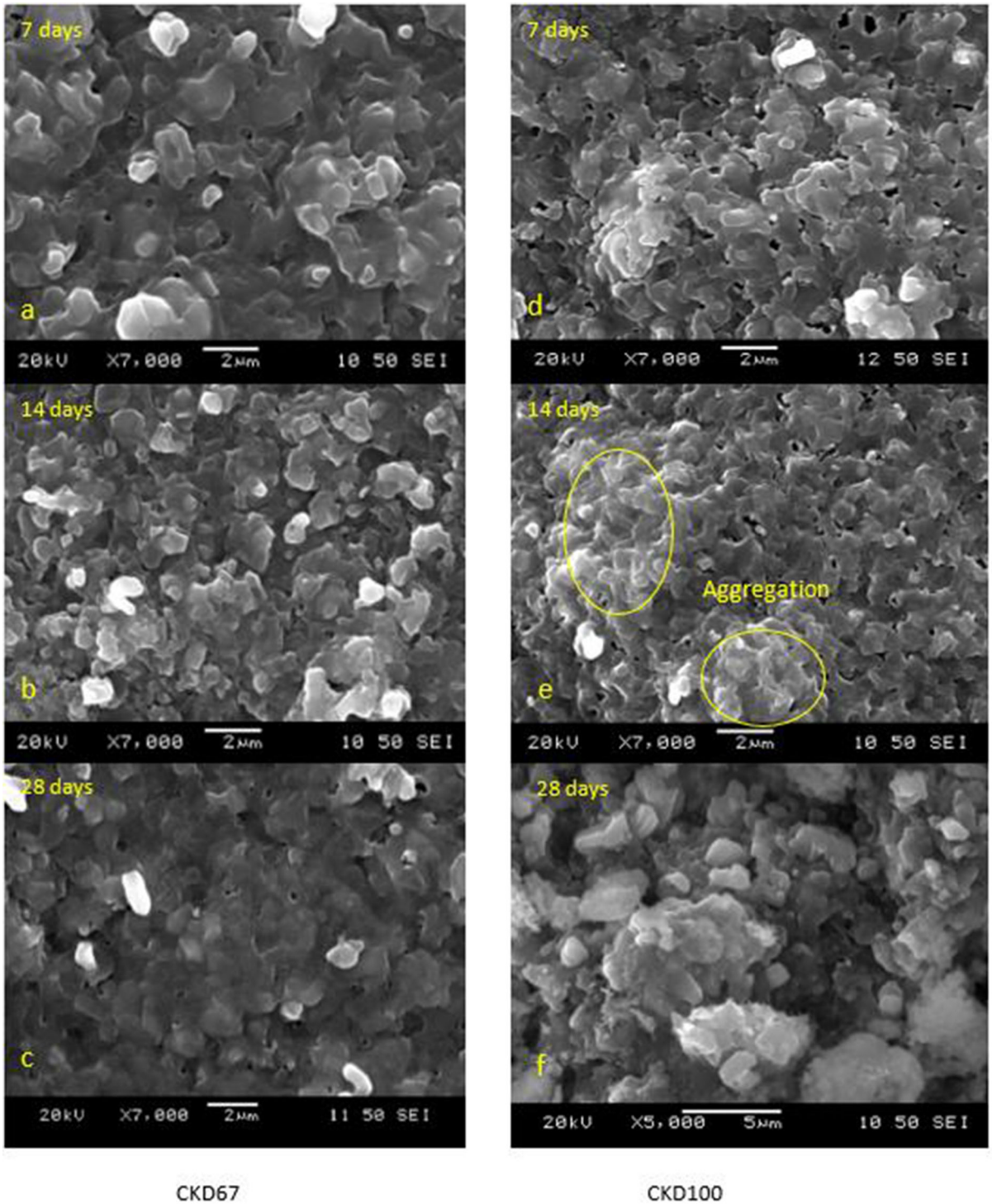

Fig. 10 SEM micrographs of clay specimens treated with CKD dosages of 67 and 100 kg/m^3

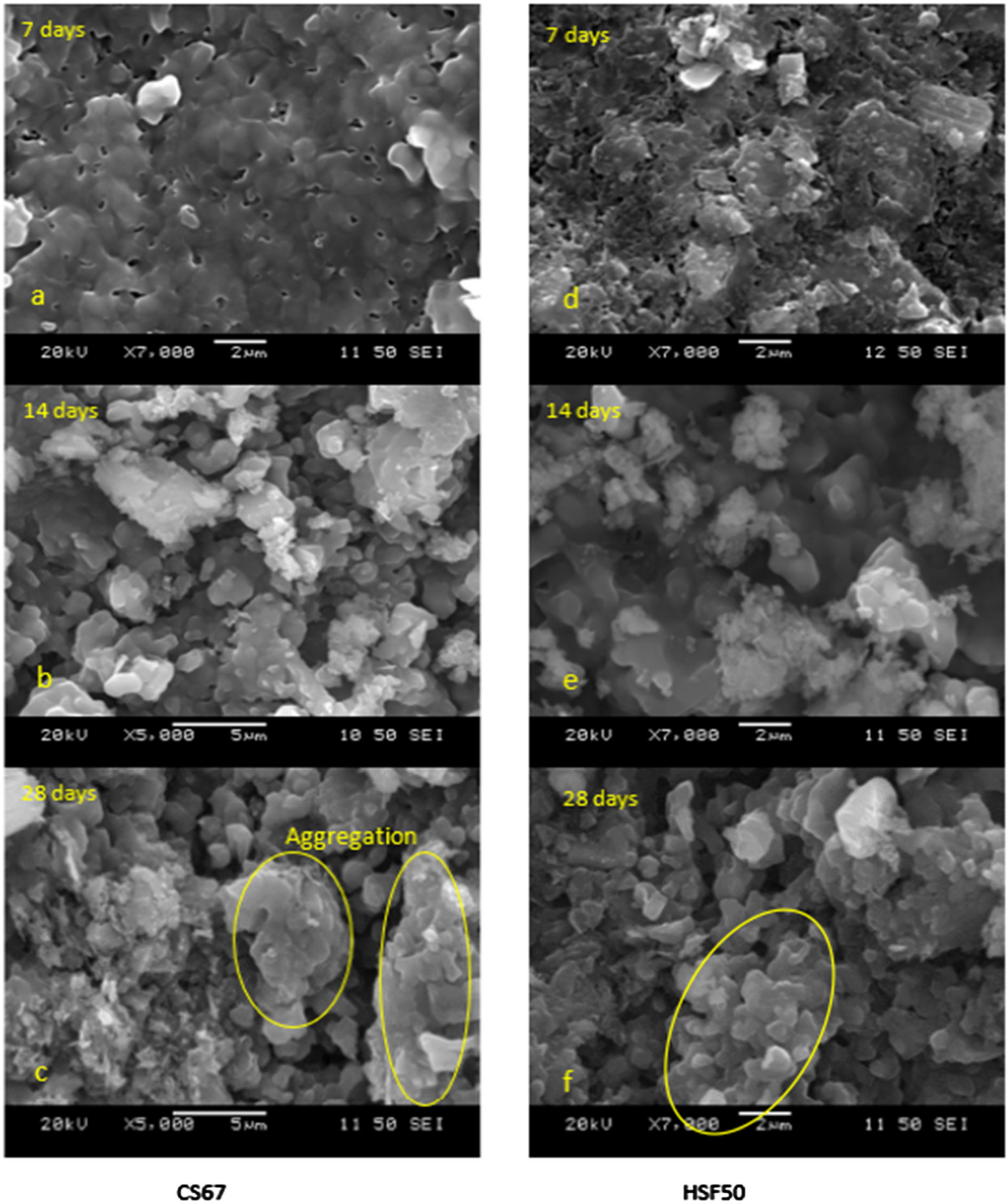

Fig. 11 SEM micrographs of clay specimens treated with CS67 and HSF50 binders

to subsequent dissolution of some silicate and aluminate from clay minerals and pozzolanic reaction. The absence of $Ca(OH)_2$ from the XRD patterns and the drop of the kaolinite and illite peaks could explain the occurrence of the pozzolanic reaction.

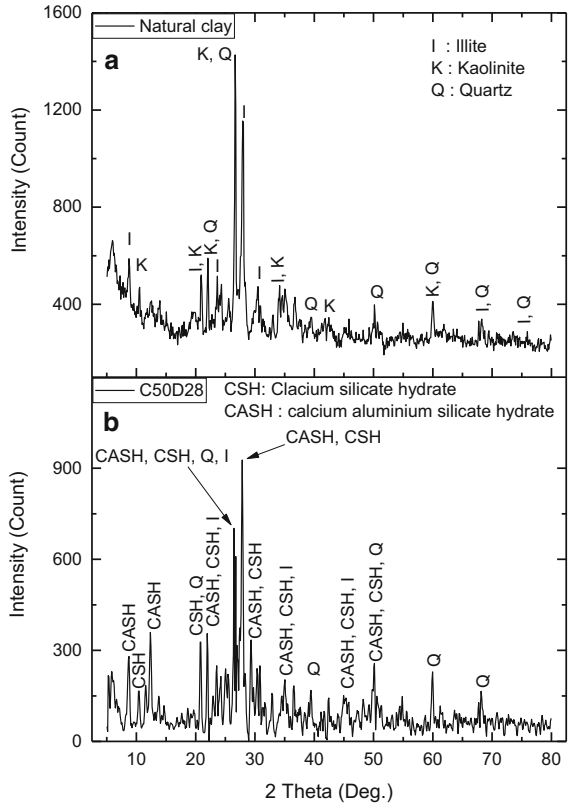

Fig. 12 XRD patterns for **a** natural clay and **b** cement-treated clay

Figure 13 shows the elemental compositions of natural clay and the cement-treated specimens (50 kg/m^3 cement and 28-day curing). It can be noted that the amount of calcium (Ca) element increased from 3.5% in natural clay to 16.9% in the cemented clay specimen. However, there was a little change in the amount of silicon and aluminium elements. The increase in the amount of calcium element in the treated specimen is due to the cementitious products, which in turn results in a strength increase observed from the UCS tests.

5 Summary and Conclusions

An experimental investigation was conducted to understand the strength development and the microstructure changes associated with Champlain Sea clay when treated with cement-based binders. A total of five different cement-based binders were applied in this study: general use Portland cement (C), a mix of cement and cement kiln dust (CKD) (1:1 by mass); a mix of cement with CKD (3:1); a mix of cement with slag (CS) (3:1); and a mix of cement and silica fume (HSF) (8%). The unconfined compressive strength tests were conducted to measure the shear strength development under different binder type, binder dosage, and curing time conditions. The scanning electronic microscopy (SEM) and X-ray diffraction (XRD) analyses were conducted to investigate the microstructural changes in the treated clay specimens. Based on the test results, the following conclusions can be drawn:

- In general, cement is efficient to treat Champlain Sea clay resulting in a significant strength increase. The optimum cement dosage was found to be around 100 kg/m^3 in terms of strength improvement and cost-effectiveness.
- Among the five different binders, cement is the most efficient in improving the shear strength of treated clay after a short curing time. The clay samples treated with CKD100 (50 kg/m^3 cement plus 50 kg/m^3 CKD) and CS67 (50 kg/m^3 cement plus 17 kg/m^3 slag) showed a substantial shear strength increase over time due to pozzolanic reaction. These results proved the feasibility and efficiency of using CKD or slag to replace a portion of cement in treating Champlain Sea clay.
- Based on the SEM observations, natural Champlain Sea clay exhibits an open structure with flocculated particles with sizes of around 1 μm. The links were observed between the microstructural changes due to artificial cementation. The SEM images of the cement-treated clay specimens indicated the presence of a reticulated matrix within the material. As the cement dosage increased, the microstructure of cement-treated clay gradually transformed from a dispersed structure into a flocculated state. The cementitious products were affixed to the particles, coated the particle surfaces, and formed large clay-binder aggregates with sizes up to 7 μm. The hydration products and cementitious products filled the voids between the aggregates and enhanced the bonding between the aggregates, which resulted in the shear strength improvement in the treated clay.
- Based on the XRD analyses, cementitious products such as calcium silicate hydrate (CSH) ($Ca_{1.5}SiO_{3.5}$. H_2O) and calcium tecto-dialumodisilicate

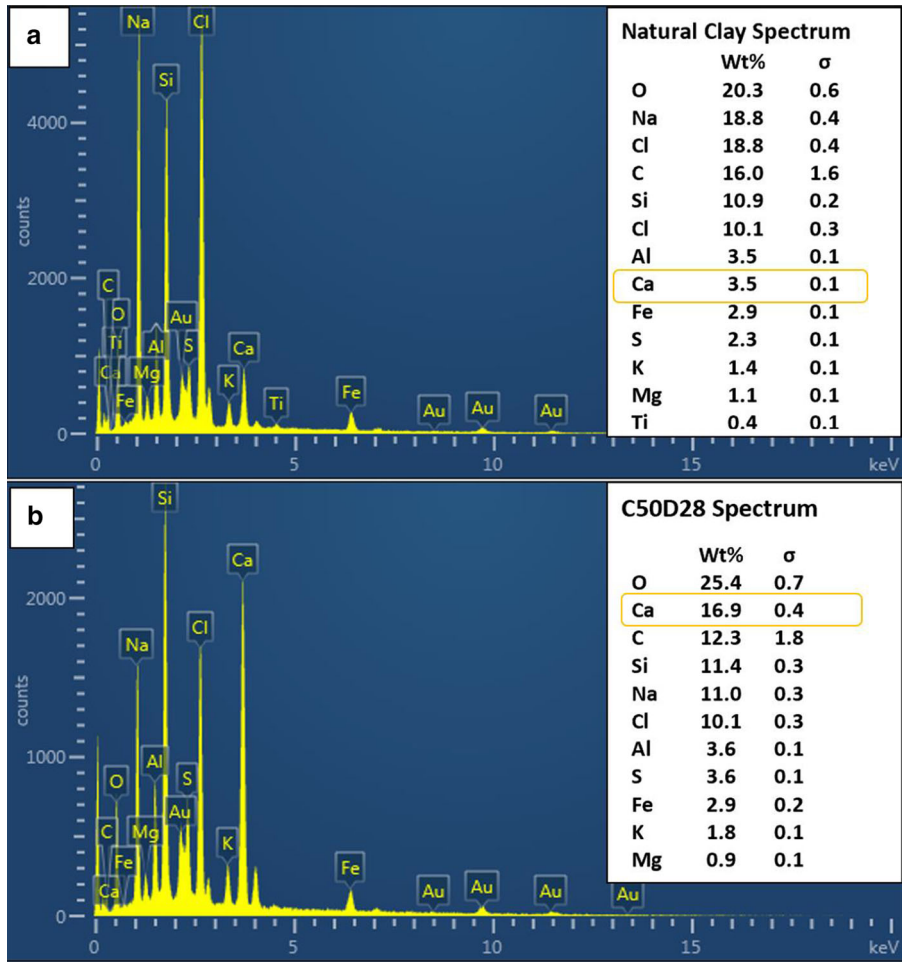

Fig. 13 Elemental compositions of **a** natural clay and **b** cement-treated clay

tetrahydrate (CASH) ($CaAl_2$ Si_2O_8 $(H_2O)_4$) were formed in the clay specimen treated by 50 kg/m^3 general use Portland cement and cured for 28 days, which explains the strength improvement of Champlain Sea clay due to cement mixing.

Acknowledgements This study was made possible with funding from the National Sciences and Engineering Research Council of Canada (NSERC) and Keller Foundations Ltd through a Collaborative and Research and Development Grant entitled "Deep Mixing to Stabilize Champlain Sea Clay." The authors would also like to acknowledge the use of undisturbed Laval samples collected by Ontario Power Generation (OPG) for its Dam Safety Program and technical help from Dr. Qiang Li at Department of Mechanical and Industry Engineering of Ryerson University. The editorial review help from Ms. Abulimiti Ayizula is greatly appreciated.

References

Afroz M, Ahmad A, Sangiuliano T, Lesage K, Cavers W, & Liu J (2018) Experimental investigation of cement mixing to improve champlain sea clay: a case study. In: GeoEdmonton 2018 CGS annual conference, Edmonton, Canada

Åhnberg H, Johansson SE, Pihl H, Carlsson T (2003) Stabilising effects of different binders in some Swedish soils. Proc Inst Civil Eng-Gr Improv 7(1):9–23

Al-Rawas AA, Taha R, Nelson JD, Al-Shab BT, Al-Siyabi H (2002) A comparative evaluation of various additives used in the stabilization of expansive soils. Geotech Test J 25(2):199–209

Baker S (2000) Deformation behavior of lime/cement column stabilized clay. Chalmers University of Technology

Bergado DT, Anderson LR, Miura N, Balasubramaniam AS (1996) Soft ground improvement in lowland and other environments. American Society of Civil Engineers (ASCE) Press, New York

Bruce M, Berg R, Collin J, Filz G, Terashi M, Yang D (2013) Federal highway administration design manual: deep

mixing for embankment and foundation support. US Department of Transportation, McLean
Chew SH, Kamruzzaman AHM, Lee FH (2004) Physicochemical and engineering behavior of cement treated clays. J Geotech Geoenviron Eng 130(7):696–706
Choobbasti AJ, Kutanaei SS (2017) Microstructure characteristics of cement-stabilized sandy soil using nanosilica. J Rock Mech Geotech Eng 9(5):981–988
Crawford CB (1968) Quick clays of eastern Canada. Eng Geol 2(4):239–265
Du YJ, Jiang NJ, Liu SY, Jin F, Singh DN, Puppala AJ (2014) Engineering properties and microstructural characteristics of cement-stabilized zinc-contaminated kaolin. Can Geotech J 51(3):289–302
Eden WJ, Fletcher EB, Mitchell RJ (1971) South nation river landslide, 16 May 1971. Can Geotech J 8(3):446–451
Fang YS, Chung YT, Yu FJ, Chen TJ (2001) Properties of soil-cement stabilised with deep mixing method. Proc ICE -Gr Improv 5(2):69–74
Gillot JE (1970) Fabric of Leda clay investigated by optical, electron-optical, and X-ray diffraction methods. Eng Geol 4(2):133–153
Horpibulsk S, Rachan R, Suddeepong A, Chinkulkijniwat A (2011) Strength development in cement admixed Bangkok clay: laboratory and field investigations. Soils Found 51(2):239–251
Horpibulsuk S, Rachan R, Chinkulkijniwat A, Raksachon Y, Suddeepong A (2010) Analysis of strength development in cement-stabilized silty clay from microstructural considerations. Constr Build Mater 24(10):2011–2021
Kamruzzaman AH, Chew SH, Lee FH (2009) Structuration and destructuration behavior of cement-treated Singapore marine clay. J Geotech Geoenviron Eng 135(4):573–589
Karrow PF(1961) The Champlain Sea and its sediments. In: Soils in Canada: geological, pedological, and engineering studies, pp 97–108
Kawasaki T (1981) Deep mixing method using cement hardening agent. In: Proceedings of 10th international conference on soil mechanics and foundation engineering, pp 721–724
Kitazume M, Terashi M (2013) The deep mixing method. CRC Press
Lee FH, Lee Y, Chew SH, Yong KY (2005) Strength and modulus of marine clay-cement mixes. J Geotech Geoenviron Eng 131(2):178–186
Li S, Kirstein A, Gurpersaud N, & Liu J (2016) Experimental investigation of cement mixing to improve Champlain Sea clay. In: GeoVancouver 2016 CGS Annual Conference, Vancouver, Canada
Liu SY, Du YJ, Yi YL, Puppala AJ (2012) Field investigations on performance of T-shaped deep mixed soil cement column–supported embankments over soft ground. J Geotech Geoenviron Eng 138(6):718–727
Liu J, Shi C, Afroz M, & Kirstein A (2017) Numerical investigation of long-term settlement of Waba dam. Technical Report, Ryerson University, Toronto, Canada
Liu L, Zhou A, Deng Y, Cui Y, Yu Z, Yu C (2019) Strength performance of cement/slag-based stabilized soft clays. Constr Build Mater 211:909–918
Locat J, Trembaly H, Leroueil S (1996) Mechanical and hydraulic behaviour of a soft inorganic clay treated with lime. Can Geotech J 33(4):654–669
Lorenzo GA, Bergado DT (2004) Fundamental parameters of cement-admixed clay—new approach. J Geotech Geoenviron Eng 130(10):1042–1050
Lorenzo GA, Bergado DT (2006) Fundamental characteristics of cement-admixed clay in deep mixing. J Mater Civ Eng 18(2):161–174
Miura N, Horpibulsuk S, Nagaraj TS (2001) Engineering behavior of cement stabilized clay at high water content. Soils Found 41(5):33–45
Monsif M, Liu J, Gurpersaud N (2020) Impact of salinity on strength and microstructure of cement-treated Champlain Sea clay. Marine Georesources & Geotechnology
Okumura T, & Terashi M (1975) Deep-lime-mixing method of stabilization for marine clays. In: Proceedings of the 5th asian regional conference on soil mechanics and foundation engineering. 1:69–75. Bangalore: Indian Institute of Science
Okumura T, Mitsumoto T, Terashi M, Sakai T, Yoshida T (1972) Deep lime mixing method for soil stabilization. Rep Port Harb Res Inst 11(1):67–106
Paniagua P, Fiskvik Bache BK, Karlsrud K, & Lund AK (2019) Strength and stiffness on lab-mixed specimens of stabilized Norwegian clays. In: Proceedings of the institution of civil engineers-ground improvement 1–35
Penner E, Burn KN (1978) Review of engineering behaviour of marine clays in Eastern Canada. Can Geotech J 15(2):269–282
Quigley RM, Gwyn QHJ, White OL, Rowe RK, Haynes JE, Bohdanowicz A (1983) Leda clay from deep boreholes at Hawkesbury, Ontario. Part I: geology and geotechnique. Can Geotech J 20(2):288–298
Ravindrarajah RS (1997) Strength evaluation of high-strength concrete by ultrasonic pulse velocity method. NDT E Int 4(30):261
Sasanian S, Newson TA (2013) Use of mercury intrusion porosimetry for microstructural investigation of reconstituted clays at high water contents. Eng Geol 158:15–22
Sayah AI (1993) Stabilization of a highly expansive clay using cement kiln dust. Ph.D. Dissertation, University of Oklahoma
Shen SL, Han J, Du YJ (2008) Deep mixing induced property changes in surrounding sensitive marine clays. J Geotech Geoenviron Eng 134(6):845–854
SNC-Lavalin (2017) Geotechnical investigation - Waba Dam. Report No. 633176. SNC-Lavalin GEM Québec Inc.
Tavenas F, Chagnon JY, Rochelle PL (1971) The Saint-Jean-Vianney landslide: observations and eyewitnesses accounts. Can Geotech J 8(3):463–478
Terashi M (1977) Chemical Soil Stabilization Methods Applicable to Port and Harbor Construction. In: Proceedings of 1977 annual research presentations of port and harbor research institute, 63–100
Terashi M, Tanaka H, Mitsumoto T, Niidome Y, Honma S (1980) Fundamental properties of lime and cement treated soils, 2nd report. Report of the Port and Harbour Research Institute, Tokyo ((**in Japanese**))

Yala IA, Agbede IO, Joel M (2012) Effect of cement kiln dust (CKD) on some geotechnical properties of black cotton soil (BCS). Electron J Geotech Eng 17(H):967–977

Yoobanpot N, Jamsawang P, Horpibulsuk S (2017) Strength behavior and microstructural characteristics of soft clay stabilized with cement kiln dust and fly ash residue. Appl Clay Sci 141:146–156

Yuksel I (2018) Blast-furnace slag. In: Waste and supplementary cementitious materials in concrete. Woodhead Publishing, pp. 361–415

Zaman M, Laguros JG, & Sayah A (1992) Soil stabilization using cement kiln dust. In: International conference on expansive soils. pp 347–351